

Donna V. Kliche, Andrew G. Detwiler, Paul L. Smith, and Roger W. Johnson  
South Dakota School of Mines and Technology, Rapid City, SD, USA

### Abstract

The parameter-fitting method of L-moments is applied to measurements of raindrop sizes collected with the two-dimensional cloud probe (2D-C) instrument on the T-28 research aircraft. We consider exponential, gamma, and lognormal approximations of the observed size distributions. The results for the fitted parameters obtained from these observations are compared with results from the alternative methods of moments or maximum likelihood, and with computer-simulated results.

### 1. Introduction

To describe analytically a raindrop spectrum collected, one has to assume first a certain mathematical distribution that could be appropriate to describe the raindrop population from which the sample was taken. The raindrop size distribution (RSD) is expressed in terms of a distribution function  $n(D)$ , which represents the number of drops per unit size interval per unit volume of space.

The most used description for the raindrop spectrum in space is the size distribution of Marshall and Palmer (1948), which is of exponential form and has two parameters:

$$n(D) = n_0 \exp(-\Lambda D), \quad (D \geq 0) \quad (1)$$

where  $D$  is the drop diameter,  $n_0$  is the value of  $n(D)$  for  $D = 0$  and  $\Lambda$  is the scale (size) parameter. In a semi-logarithmic plot, equation (1) becomes the graph of a straight line with  $\Lambda$  as slope and  $n_0$  as the  $y$ -intercept. However, the exponential distribution is not able to describe the variety of the observed spectra (Waldvogel and Joss, 1970; Waldvogel, 1974; Joss and Gori, 1978; Ulbrich, 1983; Steiner and Waldvogel, 1987; Tokay *et al.*, 2002; Lee and Zawadzki, 2005). Use of the gamma distribution (Ulbrich, 1983; Willis, 1984), which seemed to give a more appropriate description of the natural variations of the observed RSDs, was therefore proposed (the exponential distribution is a special case). A gamma RSD can be expressed by

$$n(D) = n_1 D^\mu \exp(-\lambda D), \quad (D \geq 0) \quad (2)$$

where  $n_1$  is related to the raindrop concentration,  $\mu$  is the dimensionless shape parameter of the distribution, and  $\lambda$  is the scale parameter. The gamma distribution is widely accepted by the radar meteorology and cloud physics communities (e.g. Wong and Chidambaram, 1985; Chandrasekar and Bringi, 1987; Koizu and Nakamura, 1991; Haddad *et al.*, 1996; Tokay and Short, 1996; Ulbrich and Atlas, 1998; Zhang *et al.*, 2003), although measurements of RSDs show that even the gamma distribution is not general enough to represent adequately the full range of observed RSDs.

Feingold and Levin (1986) used another function to represent RSD, i.e., the three-parameter lognormal distribution. The lognormal distribution is related to the normal distribution through the fact that it involves a logarithmic transformation of the data, with the assumption that the resulting transformed data are described by a normal distribution (Wilks, 1995; Cerro *et al.*, 1997). In terms of raindrop diameters, the lognormal distribution can be written as

$$n(D) = \frac{N_T}{D \ln \sigma \sqrt{2\pi}} \exp \left\{ -\frac{1}{2} \left[ \frac{\ln(D/D_g)}{\ln \sigma} \right]^2 \right\}, \quad (D \geq 0) \quad (3)$$

where  $N_T$  is the total number concentration;  $D_g$  is the scale parameter, which represents the geometric mean of the raindrop diameters (or median diameter) and is defined by

$$\ln(D_g) = E[\ln(D)]. \quad (4)$$

The dimensionless shape parameter,  $\ln \sigma$ , is the standard deviation of the natural log of the raindrop diameters (standard geometric deviation) and is defined by

---

Corresponding author address: Dr. Donna V. Kliche, SDSM&T, 501 East Saint Joseph St., Rapid City, SD 57701-3995; E-mail: donna.kliche@sdsmt.edu

$$\ln \sigma = \sqrt{E[(\ln D - \ln D_g)^2]}. \quad (5)$$

Typically, in statistical literature the notation for the lognormal shape parameter is  $\sigma$  rather than  $\ln \sigma$ , but the meaning is the same with (5).

Regardless of the function chosen to represent the RSD, some means of determining the parameters appropriate for any given set of observations is needed. Apart from fitting by eye, as in Marshall and Palmer (1948), possibilities include the method of moments, the method of maximum likelihood (ML), and the L-moment method. These three methods and the corresponding equations in the case of the gamma distribution are discussed in detail in Kliche *et al.* (2007a).

## 2. Data

During T-28 Flight 817 (28 July 2003), the precipitation particles were imaged with a PMS optical array probe (2D-C). This probe produces shadow images of precipitation-size particles with a vertical window height of 0.8 mm and a pixel resolution of 0.025 mm. A brief discussion of the T-28 probe is given in Detwiler and Hartman (1991). One important limitation of this probe is its poor sampling capability in the diameters range  $< 0.2$  mm (due to optical and resolution problems) as well as in the larger sizes due to the small volume sampling capability ( $0.05 \text{ m}^3/\text{km}$ ). This probe performed well during this flight, and an example of the recorded data is shown in Figure 1.

This research flight originated in Greeley, in the northeast corner of the state of Colorado, USA, in the western High Plains of North America. The terrain is rolling short grass prairie. The target of the flight was a disorganized group of thunderstorms with echo tops reaching 12 km MSL. The aircraft conducted a series of passes through rain shafts at an altitude of 3 km MSL, roughly 1.5 km AGL and just below cloud base. Cloud base temperature was  $10^\circ\text{C}$  and the temperature at flight level was about  $12^\circ\text{C}$ . Polarimetric radar showed peak echo magnitudes of 50 dBZ, and  $Z_{dr}$  ranging from zero to one dB, at altitudes above the  $0^\circ\text{C}$  level. A distinct bright band was visible at 4.7 km

MSL (3.2 km AGL) in the stratiform regions down-shear of the convective cores. These observations are consistent with precipitation formation in the convective region producing the rainshafts by the growth of graupel through the riming of ice crystals and crystal aggregates, with melting to rain below cloud.

We selected one minute of the data collected, from 21:44:29 to 21:45:31 UTC. We considered samples each taken during 5 seconds of flight, i.e. about 500 meters traveled by the T-28 aircraft. A total of 13 samples were acquired from the data collected during the one minute interval. We selected only particles that were equal to or greater than 3 pixels in size (i.e., 0.075 mm or larger); we refer to the samples as being “censored.” The diameters for particles that were only partially imaged by the probe were determined based on an algorithm described in Detwiler and Hartman (1991). The effective sample volume varies with the particle diameter, but the data have not yet been adjusted to account for that fact. Table 1 shows the number of drops collected, and the minimum and maximum drop diameter, for each sample. The sample sizes correspond (with only one exception) to the medium sample size classification ( $20 \leq N_T < 100$ ), based on the classification described in Kliche *et al.* (2006).

## 3. Method of Analysis

The process has to begin with assuming some form for the drop size distribution function, say, exponential, gamma or logarithmic. For example, given a measured sample of drops, one may assume that an exponential distribution should describe analytically the raindrop spectrum. The next step is to estimate the parameters for the assumed distribution using the sample data.

The traditional approach with experimental RSD data has been to use the *method of moments* to estimate the parameters for the RSDs. The moments calculated from the sample data can be used to estimate the parameters of the assumed underlying exponential (or gamma or lognormal) distributions. In Kliche *et al.* (2007a) the three-moment combinations  $M_2M_3M_4$ ,  $M_2M_4M_6$  and

Buffer image: from 21:45:17.996 to 21:45:18.999 Duration: 1.003 s Distance: 100 m



**Figure 1:** Example of the 2D-C recorded data during T-28 Flight 817 (28 July 2003). The duration for this buffer was 1.003 s and the distance traveled by the airplane during this time is about 100 m.

**Table 1:** Summary of the T-28 Raindrop Samples

Sample #	Number of drops	Minimum Diameter [mm]	Maximum Diameter [mm]	Sample #	Number of drops	Minimum Diameter [mm]	Maximum Diameter [mm]
1	44	0.075	2.875	8	87	0.075	2.550
2	78	0.075	3.756	9	67	0.075	1.750
3	32	0.075	0.900	10	81	0.075	3.381
4	100	0.075	2.350	11	80	0.075	2.800
5	107	0.075	2.075	12	95	0.075	2.375
6	67	0.075	1.156	13	18	0.075	4.450
7	99	0.075	4.100				

$M_3M_4M_6$ , where  $M_i$  represents the  $i$ th moment of the distribution, are discussed in detail, and the corresponding equations for the gamma estimators are also given. The exponential case is presented in detail in Smith and Kliche (2005) and Smith et al. (2005).

However, the moment method is known to be biased (Robertson and Fryer, 1970; Wallis, 1974; Haddad et al., 1996, 1997; Smith and Kliche, 2005; Uijlenhoet et al., 2006), which means that the fitted functions often do not correctly represent the raindrop populations, and sometimes not even the samples. Smith and Kliche (2005), Smith et al. (2005), Kliche et al. (2006) and Kliche et al. (2007a) describe that the skewness in the sampling distributions of the RSD moments is the main cause for this bias. The bias is stronger when higher-order moments are considered in calculating the parameters of the “fitted” functions, and the combination of 2<sup>nd</sup>, 3<sup>rd</sup>, and 4<sup>th</sup> moments typically gives the smallest bias for three-parameter distributions. (Although lower-order moments would be desirable in such estimations, they can be poorly determined because of instrumental deficiencies.)

A second approach with experimental RSD data would be to use the *maximum likelihood* (ML) *method* to estimate the parameters for the RSDs. For the exponential distribution the ML method is equivalent to the moment method (if the zeroth and first moments are used); in the case of the gamma or lognormal distribution, the calculation of the maximum likelihood estimators requires more effort. The steps to be followed in using this method and the corresponding equations for the

gamma distribution are given in Kliche et al. (2007a).

A third approach with the data would be to use the L-moment method (Hosking and Wallis, 1997), which has been used for the first time for RSDs by Kliche et al. (2006). The L-moment approach is typically superior to ML with small samples. The corresponding equations for the gamma RSD case are given in Kliche et al. (2007a). In the case of the exponential distribution the moment (with  $M_0$  and  $M_1$ ), ML and L-moment methods are identical (Hosking and Wallis, 1997).

We applied each of these methods for the 13 samples listed in Table 1. We assumed that the samples come from drop populations that can be described by an exponential, gamma or lognormal RSD.

#### 4. Results for Assumed Exponential Distributions

Table 2 gives the mean, median, and standard deviation values for the 13 scale parameter estimates using the moment, ML and L-moment methods, in the case of assuming that the drop samples came from *exponential* RSD. Comparing the values obtained for the scale parameter, it is obvious that higher order moments give larger estimates; according to Smith and Kliche (2005), the best moment estimators are ones derived using the lower order moments. In the case of ML or L-moment estimators, the expectation is to get results with essentially no bias for samples of these sizes (Kliche et al., 2006). Those estimators also yield the smallest standard deviation.

**Table 2:** Mean, median and standard deviation of the estimated scale parameters ( $\text{mm}^{-1}$ ) for *exponential* distributions using the moment, ML and L-moment methods. The first column lists the moment pair used for the moment estimates.

Estimator	Mean	Median	Standard Deviation
$M_2M_3$	2.25	2.26	1.08
$M_3M_4$	2.44	2.36	1.29
$M_3M_6$	2.76	2.53	1.51
ML / L - moment	2.46	2.33	0.55

A probability plot for the combined samples using the exponential distribution model is shown in Figure 2. The data plotted against this distribution, if valid, are expected to give an approximately straight line; any departure from the straight line is an indicator of the departure from this distribution. Three blue lines which are very close to each other in this figure show the fitted distribution (center blue line) and the 95% confidence intervals (blue lines to the left and right of the center blue line). The points to the right of the blue lines, in the lower half of the plot, indicate that there are fewer data in the small diameter region than one would expect based on the exponential distribution. The points to the right of the lines, in the upper half of the plot, indicate that there are more data in the large diameter region than expected. The output table on the right side of the graph gives the mean drop size of 0.423 mm (for the  $N = 955$  drops), the Anderson-Darling (AD) test statistic value of 18.794 and p-value  $< 0.003$ .

We calculated the probability plot correlation coefficient (PPCC), which is also a measure of the goodness of the fit, for the exponential distribution having the scale parameter of  $2.365 \text{ mm}^{-1}$  (inverse of the mean value indicated in Figure 2). The value for the PPCC in this case is 0.979.

## 5. Results for Assumed Gamma Distributions

In the case of assuming that the drop samples came from *gamma* RSDs, Table 3 summarizes the corresponding estimated values for the shape and scale parameters using the methods of moments, maximum likelihood and L-moments. The results for the gamma case appear consistent with our

findings (see also Kliche et al., 2007a) that the moment estimators give substantial bias, when compared to ML or L-moments; the bias is larger when higher order moments are used in the estimators. In addition, the standard deviations when ML or L-moments are applied are much smaller than in the case of the moment estimators. The findings of Kliche et al. (2006) suggest that the shape parameter of the gamma distribution tends to be overestimated by all methods; the ML and L-moment methods give superior results to moment estimators, with slightly better results given by the L-moment method with these sample sizes. For the samples collected, the L-moment estimators indicate that the shape parameter is about zero (even after adjusting for sample-volume variations), which would correspond to the special case of the gamma distribution, i.e., exponential distributions. However, the probability plot for the exponential model (Fig. 2) seems to disagree with the findings through the L-moment estimator.

The probability plot for the gamma distribution model is shown in Figure 3. In the lower half of the plot to the right of the blue lines, the red points indicate that there are fewer data in the left tail than one would expect based on the gamma distribution. The points to the right of the lines, in the upper half of the plot, indicate that there are more data in the right tail than expected. The output table on the upper right corner of the graph gives the estimated parameters: the estimated shape parameter is  $\hat{\mu} = 0.198$ , and the estimated scale parameter is  $\hat{\lambda} = 2.833$ , the Anderson-Darling test statistic value is 20.765 and p-value  $< 0.005$ , for the sample of 955 drops. In this case the calculated PPCC value is 0.972.

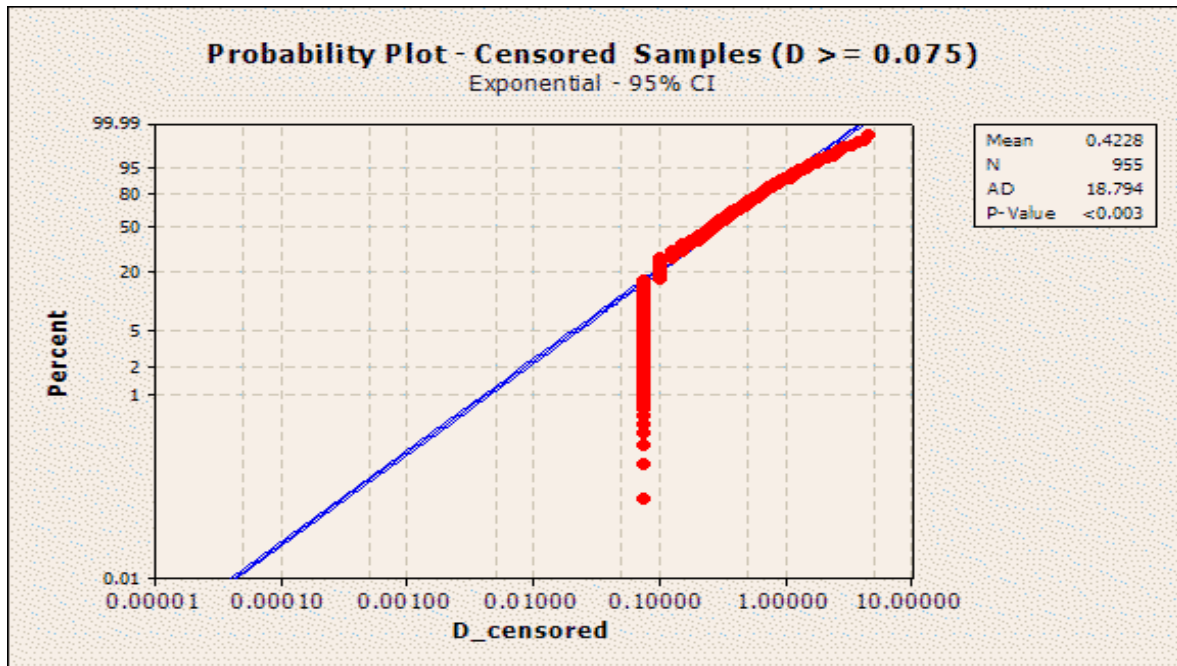


**Figure 2:** Probability plot of the data (red) against an assumed exponential distribution. The three blue lines represent the fitted distribution (centered blue line) and the confidence interval lines (to the right and left of the centered line). Population RSD: assumed to be exponential. The “D-censored” refers to the sample having drop diameter  $D \geq 0.075$  mm.

**Table 3:** Mean, median and standard deviation of the estimated shape ( $\hat{\mu}$ ) and, in parentheses, scale ( $\hat{\lambda}$ ) parameters for the *gamma* distributions using the moment, ML and L-moment methods.

Estimator	Mean	Median	Standard Deviation
$M_2M_3M_4$	2.12 (3.97)	1.21 (2.75)	2.95 (3.90)
$M_2M_4M_6$	6.80 (6.71)	3.89 (4.50)	9.53 (7.40)
$M_3M_4M_6$	18.94 (10.72)	6.02 (5.37)	42.10 (13.27)
<i>ML</i>	0.27 (3.22)	0.23 (2.87)	0.25 (1.22)
<i>L – moment</i>	-0.01 (2.51)	-0.01 (2.19)	0.27 (1.08)

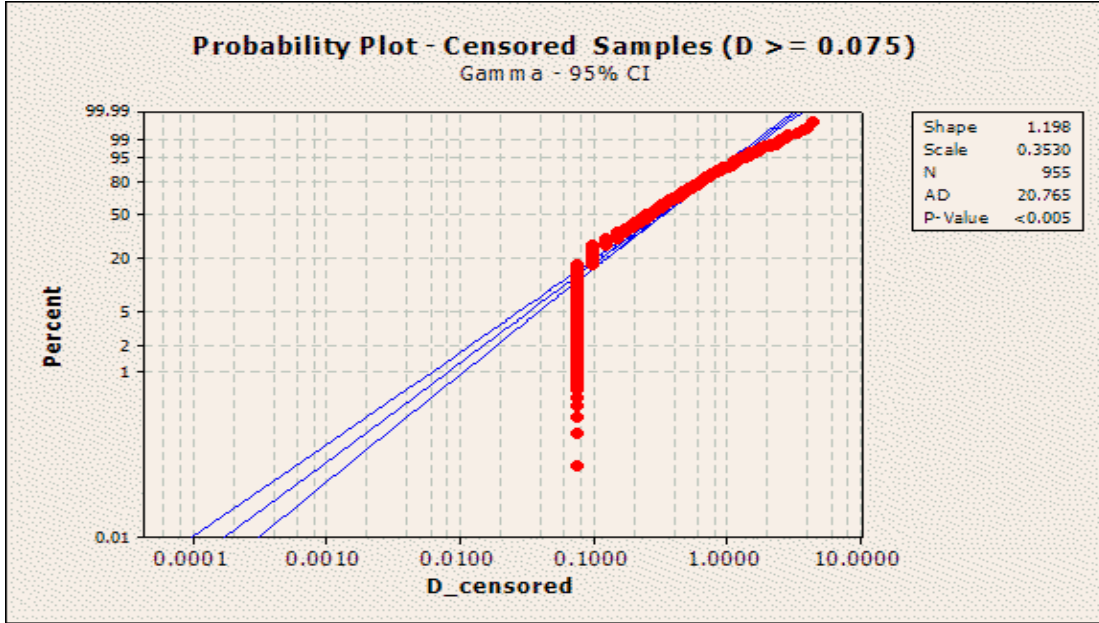


**Figure 3:** Probability plot of the data (red) against an assumed gamma distribution. The three blue lines represent the fitted distribution (centered blue line) and the confidence interval lines (to the right and left of the centered line). The shape parameter estimate given in the box is  $(1 + \hat{\mu})$ , and the scale parameter estimate is  $1/\hat{\lambda}$ . Population RSD: assumed to be gamma. The “D-censored” refers to the sample having drop diameter  $D \geq 0.075$  mm.

With the data shown in the probability plots for exponential and gamma approximations, one could conclude that the measured raindrop sample probably cannot be approximated by either exponential or gamma distributions. However, the fit shown in Figure 2 seems to be superior to the one shown in Figure 3. The left tail in Figure 2 is caused by a lack of sufficient small drops in the data, but it is also due to the truncation imposed by us for the smaller drop diameters ( $D \geq 0.075$ ), and by the pixel quantification of the drop sizes.

## 6. Results for Assumed Lognormal Distributions

Similarly, we assumed that the population from which the samples were taken could be described by the *lognormal* function (3). Table 4 gives the mean, median, and standard deviation values for the shape and scale estimators using the methods of moments, maximum likelihood and L-moments. In the case of the lognormal distribution (Kliche, 2007), the ML and L-moment methods should give results without significant bias.

**Table 4:** Mean, median and standard deviation of the estimated shape ( $\ln \hat{\sigma}$ ) and, in parentheses, scale ( $\hat{D}_g$ ) parameters for the *lognormal* distribution using the moment, ML and L-moment methods.

Estimator	Mean	Median	Standard Deviation
$M_2M_3M_4$	0.45 (1.02)	0.46 (0.75)	0.09 (0.75)
$M_2M_4M_6$	0.34 (1.34)	0.35 (1.01)	0.08 (0.89)
$M_3M_4M_6$	0.29 (1.56)	0.30 (1.10)	0.08 (0.99)
ML	0.93 (0.27)	0.90 (0.27)	0.09 (0.05)
L - moment	0.98 (0.26)	0.96 (0.26)	0.12 (0.05)

The mean value for the shape parameter from the ML and L-moment methods in Table 4 is about 0.9-1.0, which represents a wide lognormal distribution with a very long tail to the right. This means that the distribution function (3) would have to be truncated at some realistic maximum diameter, and the estimators recalculated accordingly. The widest lognormal distribution discussed by Kliche (2007) had a shape parameter of 0.5; therefore, for the purpose of this work, only the gamma distribution form was studied in further detail.

### 7. Results for Individual Samples

For each 5 s sample we consider here, the gamma RSD parameters were calculated using the two moment combinations,  $M_2M_3M_4$ , and  $M_3M_4M_6$ , as well as the ML and L-moment estimators. Figure 4 shows a comparison of cumulative histograms of the estimates of the *scale parameter*  $\lambda$  for a gamma RSD. This and the next figure demonstrate how the increase of the sampling skewness with the moment order translates into greater biases for the estimated parameters when higher-order moments are used. The  $M_2M_3M_4$  combination seems to agree well with the ML or L-moment estimators, except for two samples.

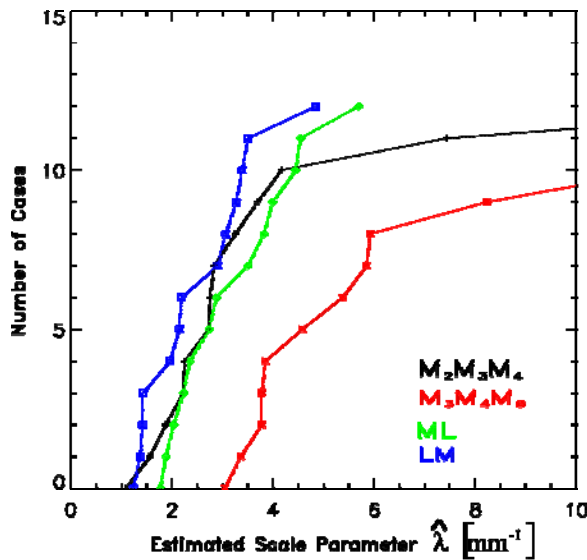


**Figure 4:** Cumulative histograms of estimated gamma scale parameter,  $\hat{\lambda}$ , using the  $M_2M_3M_4$  set (black),  $M_3M_4M_6$  set (red), ML (green) and L-moments (blue). Population RSD: assumed to be gamma.

The corresponding cumulative histograms for the estimated gamma shape parameter ( $\hat{\mu}$ ) are given in Figure 5. This figure demonstrates again that larger bias is given by using higher order moments. Based on our findings (Kliche, 2007), both the ML and L-moment estimators should be the closest to the true population value; they suggest a value not far different from zero (i.e., an exponential RSD) for each individual sample.

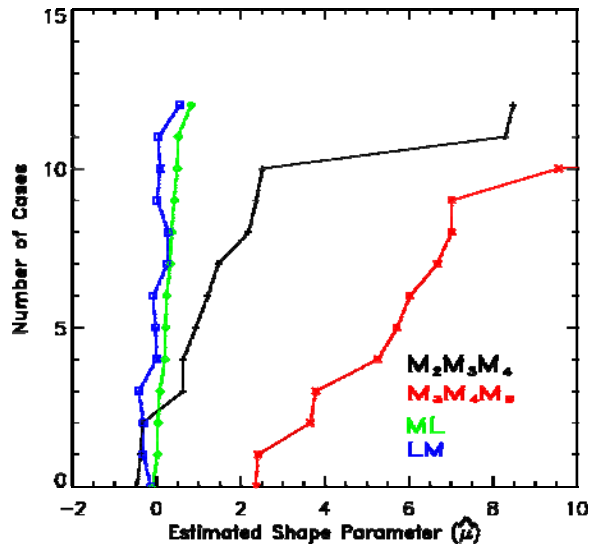


**Figure 5:** Cumulative histograms of estimated gamma shape parameter,  $\hat{\mu}$ , using the  $M_2M_3M_4$  set (black),  $M_3M_4M_6$  set (red), ML (green) and L-moments (blue). Population RSD: assumed to be gamma.

### 8. Results for Composite Sample

Figure 6 gives the composite histogram of all the drops from the samples collected during the one minute flight segment (955 drops). Overlaid distributions correspond to the estimated RSD parameters using the L-moment, ML and moment methods. The continuous red line corresponds to the  $M_3M_4M_6$  case, the continuous green line, dotted red line and dash-dot red line (which all coincide) correspond to ML,  $M_2M_3M_4$  and  $M_2M_4M_6$  respectively. The blue line corresponds to the L-moments case. Even though the curves differ, it appears from this figure, that all the estimators give comparable results over the range of sizes included in the analysis. This is not a surprise, since the composite sample (from adding all 13 samples collected during one minute of T-28 flight) consisted of 955 drops. Based on the results described in Kliche *et al.* (2007a), when large enough samples are available the three fitting

methods are expected to give comparable results. A suitable goodness-of-fit test would be needed to discriminate among these estimators.

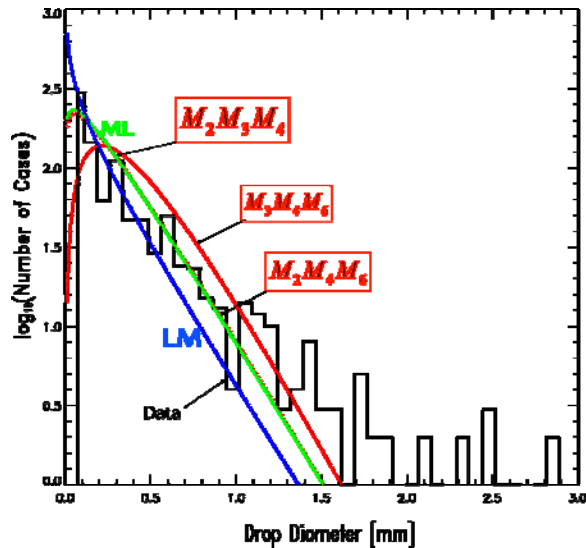


**Figure 6:** Histogram corresponding to the T-28 data collected during 21:44:29 to 21:45:31 UTC (955 drops); curves using the gamma PDF function (Kliche *et al.*, 2007a) from the parameters using the L-moment ( $\hat{\mu}_{LM} = -0.01$ ), ML ( $\hat{\mu}_{ML} = 0.27$ ) and moment (shape parameter:  $M_2M_3M_4 = 2.12$ ;  $M_2M_4M_6 = 6.8$ ;  $M_3M_4M_6 = 18.94$ ) fitting methods.

### 9. Correlation Issues

The correlations between the sample moments and the maximum drop diameter  $D_{max}$  in the sample were the first correlations investigated. Figure 7 shows an example of such correlation, for the case of the 6<sup>th</sup> moment (proportional to reflectivity factor); these are individual samples, not necessarily from the same population, but a similar correlation with nearly identical correlation coefficient showed up in the simulations of repetitive sampling from an exponential RSD with mean sample size 100 drops (Kliche, 2007).

The sample moments are also correlated with each other; Figure 8 shows such a correlation between the 3<sup>rd</sup> and 6<sup>th</sup> sample moments. The slope of this relationship would correspond to an exponent 2.44 in the “Z-W” relationship, but this “relationship” may be due here only to the variabil-

ity in the samples taken from a common raindrop population.

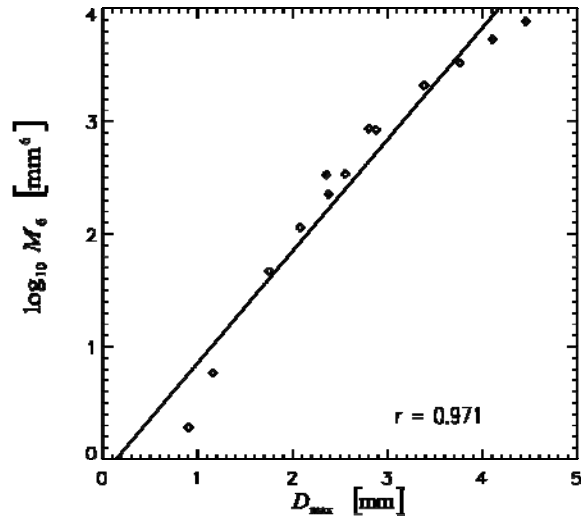


**Figure 7:** Scatter plot of 6<sup>th</sup> sample moment values versus the maximum drop diameter in the sample; the correlation coefficient is 0.971.

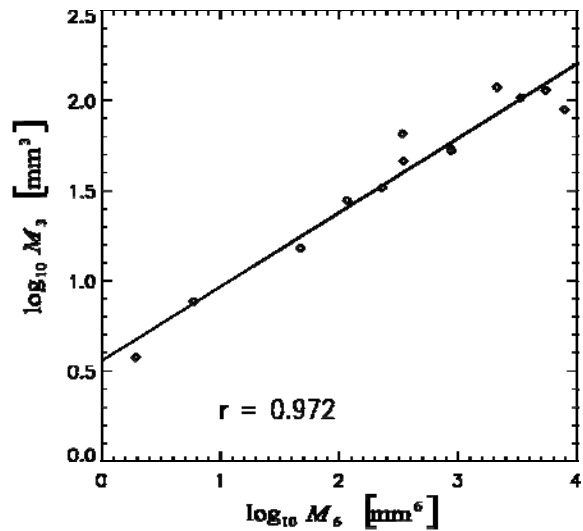


**Figure 8:** Scatter plot of 3<sup>rd</sup> versus 6<sup>th</sup> sample moment values; the correlation coefficient is 0.972.

The correlations of the various sample moments with the maximum drop size in a sample, and the associated correlations between moments, lead to correlation of the “fitted” gamma parameters with the maximum drop size. Figure 9 shows the correlation between the mass-weighted



mean diameter estimates ( $\hat{D}_m$ ) and the maximum drop diameter in the samples. This figure provides a comparison between the estimated values using the moments  $M_3M_4M_6$  with ones from the ML and L-moment estimators.

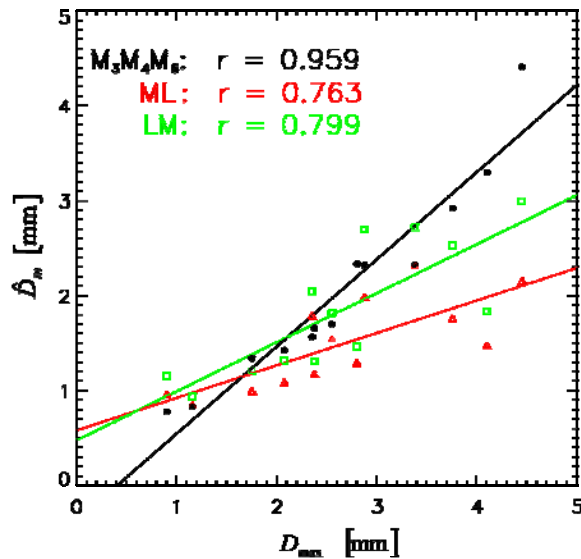


**Figure 9:** Scatter plot of estimated mass-weighted mean diameter ( $\hat{D}_m$ ) versus the maximum diameter in the samples:  $M_3M_4M_6$  (black,  $r = 0.959$ ), ML (red,  $r = 0.763$ ), L-moments (green,  $r = 0.799$ ).

A second example of such correlations is shown in Figure 10 for the normalized concentration parameter  $\hat{N}_W$  (defined in Bringi and Chandrasekar, 2001) and the maximum drop size in the sample. The correlations in the case of the ML and L-moment estimators are weaker than in the case of the moment estimators.

Correlations also exist between the estimated parameters; results from simulations of repetitive sampling (Kliche, 2007) suggest that one should be very cautious in inferring any physical relationships between such “fitted” parameters. Figure 11 gives examples of such correlations between the mass-weighted mean diameter ( $\hat{D}_m$ ) versus total number concentration ( $\hat{N}_T$ ), in the case of  $M_2M_3M_4$  and  $M_3M_4M_6$  estimators as compared to the ML and L-moment estimators. The ML and L-moment estimators are correlated, but their correlation is weaker than in the case of the moment estimators, and is not significant under an assumption of normally-distributed residuals.

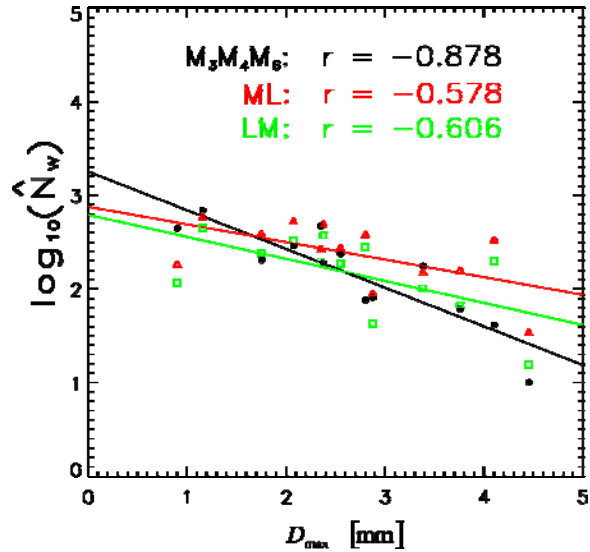


**Figure 10:** Scatter plot of the estimated normalized concentration parameter ( $\hat{N}_W$ ) versus the maximum diameter in the samples:  $M_3M_4M_6$  (black,  $r = -0.878$ ), ML (red,  $r = -0.578$ ), LM (green,  $r = -0.606$ ). Population RSD: assumed to be gamma.

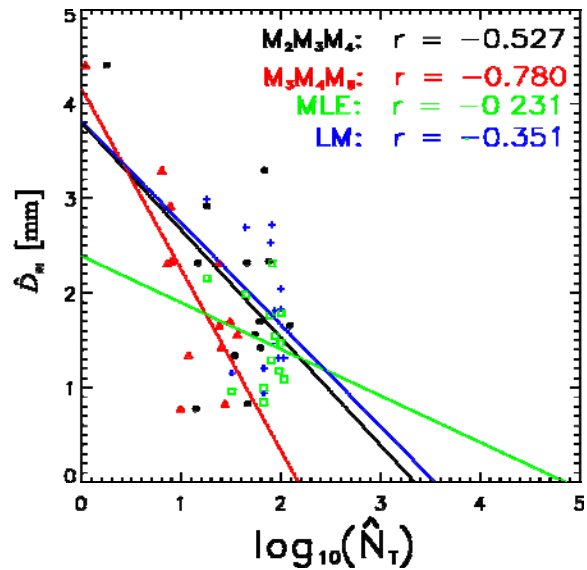


**Figure 11:** Scatter plot of the estimated total number concentration parameter ( $\hat{N}_T$ ) versus the mass-weighted mean diameter ( $\hat{D}_m$ ):  $M_2M_3M_4$  (black,  $r = -0.527$ ),  $M_3M_4M_6$  (red,  $r = -0.780$ ), ML (green,  $r = -0.231$ ), L-moments (blue,  $r = -0.351$ ). Population RSD: assumed to be gamma.

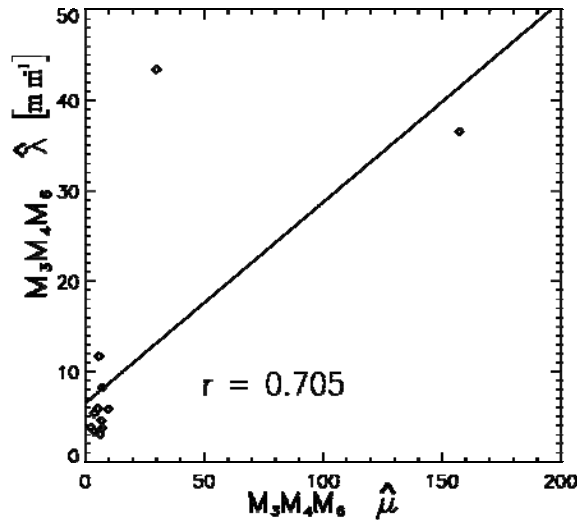


**Figure 12:** Scatter plot of the estimated  $M_3M_4M_6$  scale parameter  $\hat{\lambda}$  vs.  $M_3M_4M_6$  shape parameter  $\hat{\mu}$ ; the correlation coefficient is  $r=0.705$ . Population RSD: assumed to be gamma. All 13 samples considered.

Special attention needs to be given to experimental data when such correlations are investigated. In many occasions one or two points in the scatter plot can affect this correlation dramatically. We show such an example for the case of the  $M_3M_4M_6$  estimators,  $\hat{\lambda}$  vs.  $\hat{\mu}$ , in Figure 12. The correlation coefficient in this case is calculated to be 0.705. However, a careful look into this graph shows two experimental points well separated from the main cluster; these points correspond to the “outlier” cases in Figures 4 and 5. Figure 13 shows the same graph as in Figure 12, with the two outlying points removed. Now the correlation is not significant.

For the L-moment and ML estimators, the  $\hat{\lambda}$  vs.  $\hat{\mu}$  correlation still exists and there is no indication of outlier points. Figure 14 gives the corresponding scatter plot for these estimators, showing a correlation of about 0.9. Simulation results in Kliche (2007) show similar correlation coefficients for the ML and L-moment,  $\hat{\lambda}$  vs.  $\hat{\mu}$  estimators, arising from repetitive sampling from the same population.

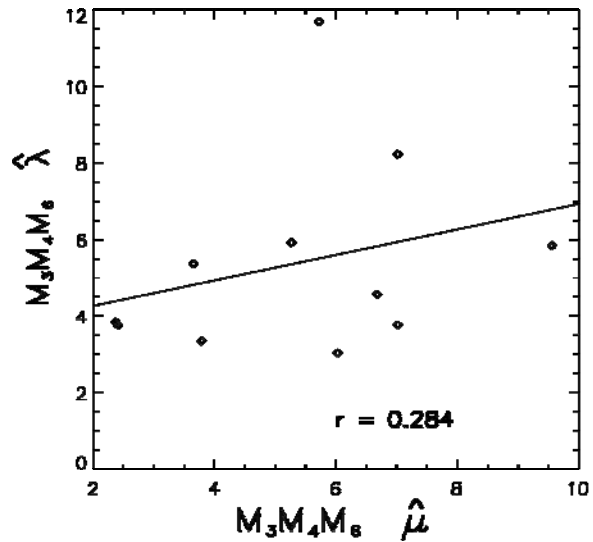


**Figure 13:** Scatter plot of the estimated  $M_3M_4M_6$  scale parameter  $\hat{\lambda}$  vs.  $\hat{\mu}$  shape parameter. Correlation coefficient is 0.284. Only 11 samples considered.

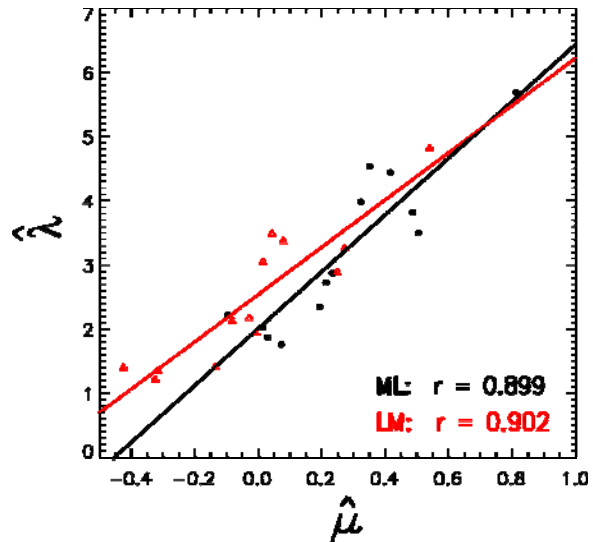


**Figure 14:** Scatter plot of the estimated scale parameter  $\hat{\lambda}$  vs. shape parameter  $\hat{\mu}$ : ML ( $r = 0.899$ ) in black; L-moments ( $r = 0.902$ ) in red. Population RSD: assumed to be gamma. All 13 samples are considered.

## 10. Conclusions

The main goal for the present work was to apply the L-moments method described in Kliche et al. (2007a) to real raindrop data collected during T-28 Flight 817, and to compare the results with findings from those simulations. The L-moments method was applied, and the results were compared to the ones obtained with the moment method and the maximum likelihood method.

As shown in Kliche *et al.* (2007a), the L-moment parameters for gamma distributions have the smallest bias of the three fitting methods studied (moments, ML, L-moments). The results for the real data used in this study appear to be consistent with those simulation results. The least biased estimators suggest that these raindrop size distributions, observed just below cloud base at about 12 °C, are approximately exponential.

*Acknowledgement:* This research work was partially supported by NSF Grant ATM-0531690.

## 11. References

- Bringi, V.N., and V. Chandrasekar, 2001: *Polarimetric Doppler Weather Radar: Principles and Applications*, Cambridge University Press, 636p.
- Cerro, C., B. Codina, J. Bech, and J. Lorente, 1997: Modeling raindrop size distributions and Z(R) relations in the Western Mediterranean area. *J. Appl. Meteor.*, **36**, 1470-1479.
- Chandrasekar, V., and V.V. Bringi, 1987: Simulation of radar reflectivity and surface measurements of rainfall. *J. Atmos. Oceanic Technol.*, **4**, 464-478.
- Detwiler, A.G. and K.R. Hartman, 1991: IAS method for 2D data analysis on PCs. Bulletin 91-5, Institute of Atmospheric Sciences, SDSM&T, 37 pp. + appendices.
- Feingold, G., and Z. Levin, 1986: The lognormal fit to raindrop spectra from frontal convective clouds in Israel. *J. Climate Appl. Meteor.*, **25**, 1346-1363.
- Haddad, Z.S., S.L. Durden, and E. Im, 1996: Parameterizing the raindrop size distribution. *J. Appl. Meteor.*, **35**, 3-13.
- Haddad, Z.S., D.A. Short, S.L. Durden, E. Im, S. Hensley, M.B. Grable, and R.A. Black, 1997: A new parameterization of the rain drop size distribution. *IEEE Transactions of Geosciences and Remote Sensing*, **35**, 532-539.
- Hosking, J.R.M. and J.R. Wallis, 1997: *Regional Frequency Analysis: An Approach Based on L-Moments*, Cambridge University Press.
- Joss, J. and E. G. Gori, 1978: Shapes of raindrop size distributions. *J. Appl. Meteor.*, **17**, 1054-1061.
- Kliche, D.V., 2007: Raindrop Size Distribution Functions: An Empirical Approach. PhD. Dissertation, SDSM&T, 211 pgs.
- Kliche, D.V., P.L. Smith and R. W. Johnson, 2006: Estimators for parameters of drop-size distribution functions: sampling from gamma distributions, *12<sup>th</sup> Conference on Cloud Physics*, Madison, WI, Amer. Meteor. Soc.
- Kliche, D.V., P.L. Smith, R.W. Johnson, 2007a: L-Moment estimators as applied to exponential, gamma, and lognormal drop size distributions. *33<sup>rd</sup> Conf. on Radar Meteorology*, Cairns, Australia, Amer. Meteor. Soc.
- Kliche, D.V., A.G. Detwiler, P.L. Smith, and R.W. Johnson, 2007b: L-Moment method applied to observed raindrop size distribution. *33<sup>rd</sup> Conf. on Radar Meteorology*, Cairns, Australia, Amer. Meteor. Soc.
- Kliche, D.V., A.G. Detwiler, P.L. Smith, and R.W. Johnson, 2007b: L-Moment method applied to observed raindrop size distribution. *33<sup>rd</sup> Conf. on Radar Meteorology*, Cairns, Australia, Amer. Meteor. Soc.
- Kozu, T., and K. Nakamura, 1991: Rainfall parameter estimation from dual-radar measurements combining reflectivity profile and path-integrated attenuation. *J. Atmos. Oceanic Technol.*, **8**, 259-270.
- Lee, G., and I. Zawadzki, 2005: Variability of drop size distributions: time-scale dependence of the variability and its effects on rain estimation. *J. Appl. Meteor.*, **44**, 241-255.
- Marshall, J. S. and W. McK. Palmer, 1948: The distribution of raindrops with size. *J. Meteor.*, **5**, 165-166.
- Robertson, C.A., and J.G. Fryer, 1970: The bias and accuracy of moment estimators. *Biometrika*, **57**, 57-65.
- Smith, P. L. and D. V. Kliche, 2005: The bias in moment estimators for parameters of drop-size distribution functions: sampling from exponential distributions. *J. Appl. Meteor.*, **44**, 1195-1205.
- Smith, P. L., D. V. Kliche and R. W. Johnson, 2005: The bias in moment estimators for parameters of drop-size distribution functions: sampling from gamma distributions. *32<sup>nd</sup> Conf. on Radar Meteorology*, Albuquerque, NM, Amer. Meteor. Soc.
- Steiner, M., and A. Waldvogel, 1987: Peaks in raindrop size distributions. *J. Atmos. Sci.*, **44**, 3127-3133.

- Tokay, A., and D.A. Short, 1996: Evidence from tropical raindrop spectra of the origin of rain from stratiform versus convective clouds. *J. Appl. Meteor.*, **35**, 355-371.
- Tokay, A., A. Kruger, W.F. Krajewski, P.A. Kucera, and A.J.P.Filho, 2002: Measurements of drop size distribution in southwestern Amazon basin. *J. Geophys. Res.*, **17**, LBA 19-1:19-15.
- Uijlenhoet, R., J.M. Porra, D.S. Torres, and J. D. Creutin, 2006: Analytical solutions to sampling effects in drop size distribution measurements during stationary rainfall: estimation of bulk rainfall variables. *J. Hydrology*, **328**, 65-82.
- Ulbrich, C. W., 1983: Natural variations in the analytical form of the raindrop size distribution. *J. Climate Appl. Meteor.*, **22**, 1764-1775.
- Ulbrich, C. W., 1985: The effects of drop size distribution truncation on rainfall integral parameters and empirical relations. *J. Climate Appl. Meteor.*, **24**, 580-590.
- Ulbrich, C.W., and D. Atlas, 1998: Rainfall microphysics and radar properties: analysis methods for drop size spectra. *J. Appl. Meteor.*, **37**, 912-923.
- Waldvogel, A., 1974: The  $N_0$  jump of raindrop spectra. *J. Atmos. Sci.*, **31**, 1067-1078.
- Waldvogel, A., and J. Joss, 1970: The influence of a cold front on the drop size distribution. *Preprints, Conf. Cloud Physics*, Ft. Collins, Colo., Amer. Meteor. Soc, 195-196.
- Wallis, J.R., 1974: Just a Moment! *Water Resources Research*, **10**, 211-219.
- Wilks, D.S., 1995: *Statistical Methods in Atmospheric Sciences*, An Introduction, Academic Press, Inc., 465p.
- Willis, P.T., 1984: Functional fits to some observed drop size distributions and parameterization of rain. *J. Appl. Meteor.*, **41**, 1648-1661.
- Wong, R.K.W., and N. Chidambaram, 1985: Gamma size distribution and stochastic sampling errors. *J. Climate Appl. Meteor.*, **24**, 568-579.
- Zhang, G., J. Vivekanandan, E.A. Brandes, R. Meneghini, and T. Kozi, 2003: The shape-slope relation in observed gamma raindrop size distributions: statistical error or useful information? *J. Atmos. Oceanic Technol.*, **20**, 1106-1119.